LBL-19653

Lawrence Berkeley Laboratory
UNIVERSITY OF CALIFORNIA

Materials & Molecular Research Division

LBL--19653

DE86 001986

Presented at the 3rd International Conference on Superconducting Quantum Devices, Berlin, Federal Republic of Germany, June 25-28, 1985

APPLICATION OF A DC SQUID TO RF AMPLIFICATION: NQR

C. Hilbert, J. Clarke, T. Sleator, and E.L. Hahn

May 1985

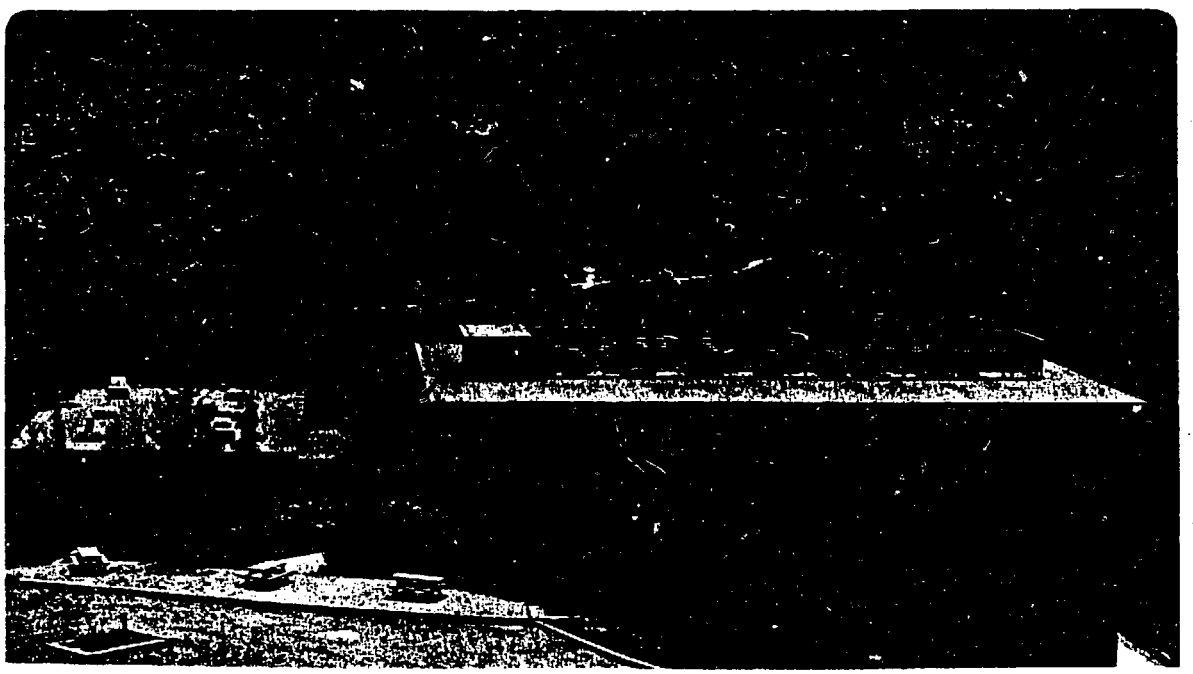

Prepared for the U.S. Department of Energy under Contract DE-AC03-76SF00098

APPLICATION OF A DC SQUID TO RF AMPLIFICATION: NQR

Claude Hilbert and John Clarke

Department of Physics, University of California and
Materials and Molecular Research Division
Lawrence Berkeley Laboratory
Berkeley, California, USA 94720

Tycho Sleator and Erwin L. Hahn

Department of Physics, University of California
Berkeley, California, USA 94720

Superconducting QUantum Interference Devices (SQUIDs) have been used for more than a decade for the detection of magnetic resonance.[1-10] Until recently, these devices had mostly been confined to operation in the audiofrequency range, so that experiments have been restricted to measurements of resonance at low frequencies,[9-10] or of changes in the static susceptibility of a sample induced by rf irradiation at the resonant frequency.[1-8] However, the recent extension[11] of the operating range of low noise dc SQUIDs to radiofrequencies (rf) allows one to detect magnetic resonance directly at frequencies up to several hundred megahertz. In this paper, we begin by summarizing the properties of dc SQUIDs as tuned rf amplifiers. We then describe first, the development of a SQUID system for the detection of pulsed nuclear quadrupole resonance[12] (NQR) at about 30 MHz and second, a novel technique for observing magnetic resonance in the absence of any externally applied rf fields.

dc SQUIDs as Tuned rf Amplifiers

Figure 1 shows a dc SQUID with loop inductance L coupled to an input circuit consisting of a signal source $V_i(t)$ of resistance R_i in series with the input coil of inductance L_i, a capacitance C_i and a pick-up coil of inductance L_p. In our application to magnetic resonance detection, $V_i(t)$ is the signal induced by the rotat-

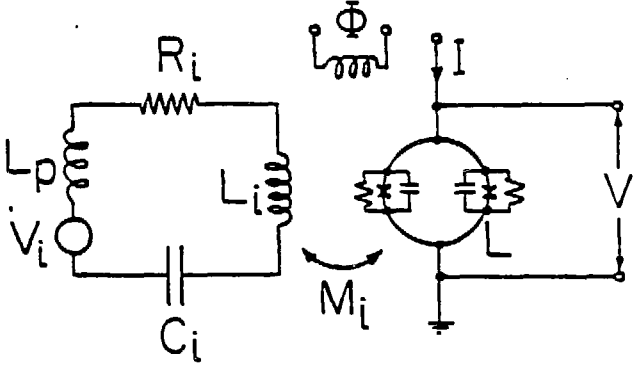

Fig. 1: Configuration of tuned amplifier based on a dc SQUID.

ing magnetization of a sample located inside the pick-up coil. The mutual inductance between the SQUID and the input coil is M_i, so that the coupling coefficient is $\alpha^2 = M_i^2/LL_i$. We also define an effective coupling coefficient between the SQUID and the input circuit: $\alpha_e^2 = M_i^2/L(L_i + L_p)$. The SQUID is biased with a current I and a flux Φ so that the flux-to-voltage transfer function, $V_\Phi \equiv \partial V/\partial\Phi$, is a maximum. In the limit $Q >> 1$, where Q is the quality factor of the input circuit, it can be shown[11] that the condition for the optimum noise temperature of a dc SQUID with $\beta \equiv 2LI_o/\Phi_o = 1$ is $R_i = \alpha^2\omega_o L_i$ or

$$Q\alpha_e^2 = 1. \qquad (1)$$

Here, $f_o = \omega_o/2\pi$ is the resonant frequency of the input circuit. This condition yields an optimum noise temperature

$$T_N(f_o) = 7\omega_o LT/R, \qquad (2)$$

a dynamic range in the bandwidth of the tuned circuit

$$D = 6Q/(T/1K), \qquad (3)$$

and a power gain at resonance

$$G(f_o) = V_\Phi/\omega_o. \qquad (4)$$

In practice, the inductive and capacitive coupling of the SQUID to the input circuit produces changes in the impedance[13]

$$\Delta R_i = - \omega_o^2 M_i V_\phi C_p L_i \qquad (5)$$

and

$$\Delta L_i = - \alpha^2 (L/\mathscr{L}) L_i , \qquad (6)$$

where C_p is the parasitic capacitance between the SQUID loop and the input coil, and $\mathscr{L}$ is the dynamic input inductance of the SQUID. These changes must be taken into account in the design of the amplifier.

The dc SQUIDs used in this work are planar, thin-film devices[11] coupled to a spiral input coil with a coupling coefficient $\alpha^2 = 0.6$. Their measured performance at 100 MHz and at a bath temperature of 4.2K is typically: $T_N = 1.7K$, $D = 1.5Q$ and $G = 20$ dB. The input circuit can be tuned to any frequency from about 1 MHz to 300 MHz.

dc-SQUID System for Detection of Pulsed NQR

The most widely used technique for the detection of magnetic resonance involves the study of the free induction decay of nuclear signals after the application of a rf-pulse to the sample.[14] Figure 2 is a schematic of our SQUID-based system for the detection of NQR. Rf pulses are amplified and coupled into a cold transmitter coil via an impedance matching circuit. The sample is located inside a pick-up coil that is connected in series with an identical oppositely-wound coil. Both coils are actually situated inside the transmitter coil, and can be adjusted to minimize their inductive coupling to the transmitter coil. In addition, a grounded Faraday shield between the transmitter and pick-up coils minimizes capacitive coupling. An optimum balance of about 3 parts in 10^5 is possible. The gradiometer-like configuration reduces the current induced into the input circuit by the rf pulses. After the rf pulse is turned off, the precessing magnetization of the sample induces a signal voltage across the pick-up coil. The pick-up coils are connected in series with an air-capacitor C_t (adjustable from the top of the cryostat), the input coil L_i of the SQUID, and

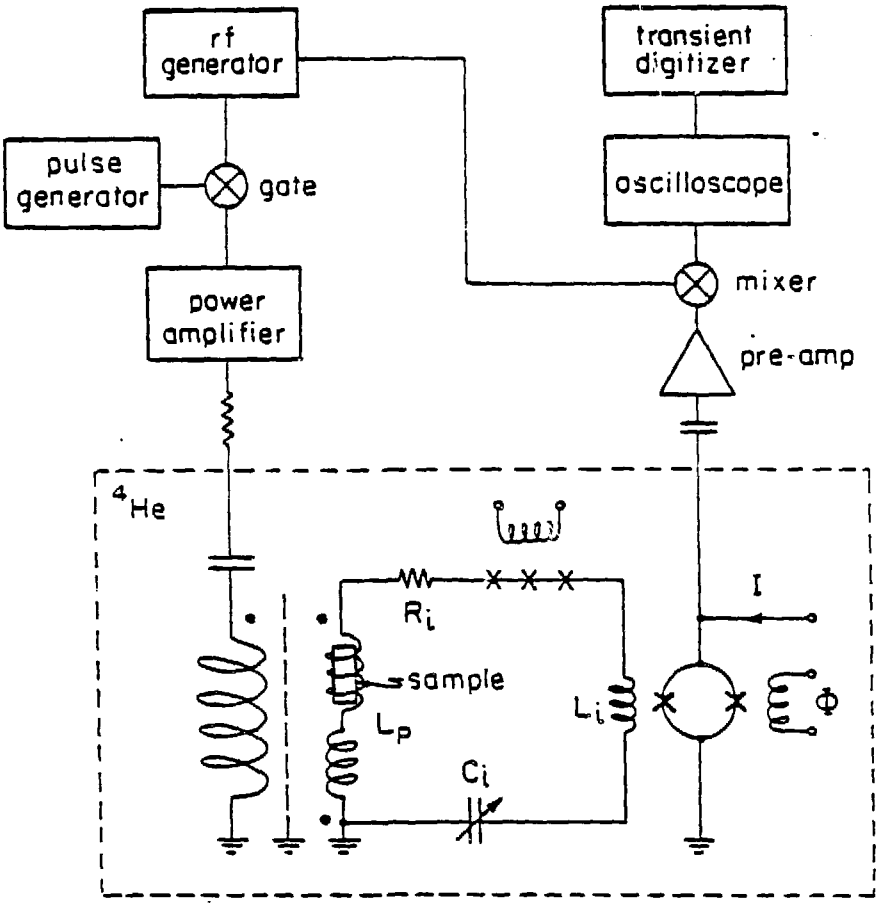

Fig. 2: Schematic layout for SQUID-based detection of NQR.

a series array of 20 Josephson tunnel junctions. The resistor R_i represents contact resistance and losses in the capacitor. The SQUID is enclosed in a superconducting Nb shield, and its output is matched to a low noise, room temperature amplifier. The amplified signal is mixed down by a double balanced mixer with a reference supplied by the rf generator. The mixed-down signal is passed through a low-pass filter and observed on an oscilloscope, and, after digitizing, stored in a computer for further analysis or averaging.

A novel feature of the input circuit is the series array of twenty 10 μm × 10 μm, Nb-NbOx-PbIn Josephson tunnel junctions. Each junction has a critical current of about 4 μA, and a hysteretic current-voltage characteristic with a resistance of about 50 Ω at voltages above the sum of the energy gaps. For signal currents below the critical current, the array has zero resistance. On the

other hand, the relatively large current induced by each rf pulse causes the junctions to switch rapidly to the resistive state with a total resistance of about 1 kΩ. Thus, the array acts as a Q-spoiler, not only providing additional protection for the SQUID but, more importantly, reducing the ring-down time of the tuned circuit after the end of the rf pulse. The quality factor Q is about 1/2 with the junctions in the resistive state. The switching threshold of the Q-spoiler, that is, the critical current of the junctions, can be varied by means of a static magnetic field applied parallel to the plane of the films.

We tested our NQR detector using approximately 0.32 cm^3 of powdered $NaClO_3$. The filling factor, referred to both pick-up coils, was 0.13. At 4.2K ^{35}Cl nuclei exhibit a quadrupole resonance at 30.6856 MHz. The spin-lattice relaxation time, T_1, was reduced to about 20 min at 4.2K by Y-ray irradiation; the spin-spin relaxation time, T_2, was 240 μs. The inductance L_i was 5.6 nH, the combined inductance L_p of the pick-up coils was 2.5 μH, and the effective coupling coefficient α_e^2 was thus about 10^{-3}. Most of the tests were performed with R_i = 0.2 Ω, yielding a Q of 2,500 at the ^{35}Cl resonant frequency. Thus, $Q\alpha_e^2$ was of the order of unity, as required for optimum operation of the amplifier [Eq. (1)]. At 4.2K with a Q of 2,500, the overall system noise temperature, including the Nyquist noise from R_i, was 6 ± 1K.

Figure 3 illustrates the mixed-down signal that follows an rf pulse. The rf signal and the resonant frequency of the tuned circuit were at the resonance of the ^{35}Cl nuclei. Figure 3 shows a single oscilloscope trace of the free induction decay following an initial nuclear spin tipping angle of 2×10^{-4} rad. The initial rms voltage induced across the pick-up coil was about 20 nV in a bandwidth of 10 kHz. By measuring the spin tipping angle required to obtain a signal-to-noise ratio of unity, we determined that the minimum number of ^{35}Cl spins observable with a single pulse in a bandwidth of 10 kHz was about 2×10^{16}. This is equivalent to about 2×10^{16} nuclear Bohr magnetons.

Figure 4 illustrates the effect of the Josephson Q-spoiler on the ring-down of a tuned circuit (Q = 100) after the rf pulses. The

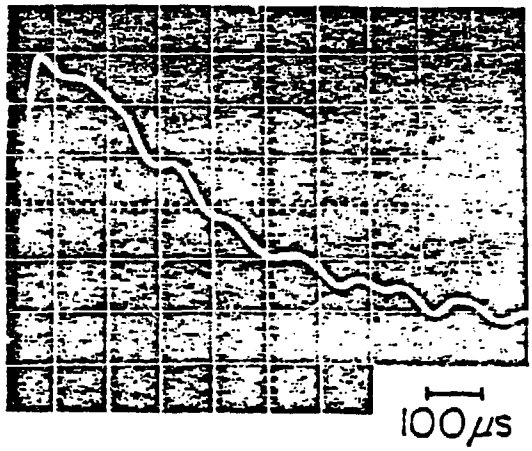

Fig. 3: Oscilloscope traces of free-induction decay of ^{35}Cl for a small signal ($\phi << \phi_c$).

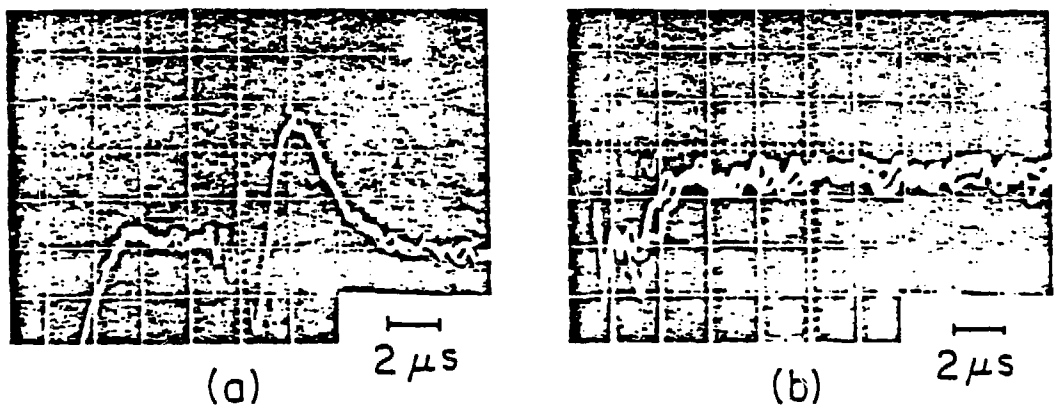

Fig. 4: Oscilloscope traces showing ring-down of tuned circuit following rf pulse, with Q = 100 (a) without Q-spoiler, and (b) with Q-spoiler.

voltage ring-down time of the circuit τ was about 1 μs at 30.5 MHz. The photographs show the mixed-down output signal, with the traces triggered at the end of the rf pulse. Figure 4(a) shows the response to a rf pulse corresponding to a peak-to-peak magnetic field of 1.5 mT at the sample, in the absence of the Q-spoiler. Figure 4(b) shows the response to the same rf-pulse in the presence of a Q-spoiler with the critical current of the junctions reduced by a magnetic field: The overall recovery time has been reduced from 17 μs to about 4 μs.

To conclude this section, we note several advantages of this system over conventional systems with room temperature amplifiers: (i) an

improvement in voltage resolution of 1 or 2 orders of magnitude, due in part to the low noise temperature of the SQUID amplifier, and in part to the high Q that the Q-spoiler allows one to use; (ii) the elimination of any amplifier dead-time; (iii) the minimization of losses in the tuned circuit; and (iv) a wide tuning range from about 1 to 300 MHz.

Thermal Noise NQR and Nuclear Spin Fluctuations

The fact that dc SQUID amplifiers can have a noise temperature comparable with or lower than the bath temperature makes possible a new means of detecting magnetic resonance. The sample is placed inside the inductor L_p of a series tuned circuit (Fig. 1), and the spectral density of the current fluctuations in the circuit is measured. In the absence of a sample, the resistance R_i produces a Nyquist current noise with a Lorentzian power spectrum. The technique consists of detecting and analyzing the departures from the Lorentzian lineshape introduced by the sample. We assume that this sample can be characterized by a complex susceptibility $\chi(\omega) = \chi'(\omega) - j\chi''(\omega)$. The impedance of the pick-up coil is modified by the sample to[14]

$$Z_p' = j\omega L_p' = j\omega L_p(1 + 4\pi\chi\xi) = j\omega(L_p + L_s) + R_s, \qquad (7)$$

where ξ is the filling factor. The presence of the spin inductance $L_s = 4\pi\chi' L_p\xi$ shifts the resonance of the circuit, while the spin resistance $R_s = 4\pi\chi''\omega L_p\xi$ modifies the damping and acts as a source of Nyquist noise.

We can compute the Nyquist noise of the spins in terms of the microscopic parameters of the sample. For all practical purposes in this experiment, the nuclear quadrupole moments interacting with local electric field gradients can be analyzed as though they were magnetic dipoles of spin 1/2 interacting with an external magnetic field B_o. In this case the splitting of the ground and excited states is $\hbar\omega_s$, where $\omega_s/2\pi = \gamma B_o/2\pi$ is the spin frequency and γ is the gyromagnetic ratio. At a spin temperature T_s, the equilibrium magnetization of the sample is:[14]

$$M_o = (n\gamma\hbar/2)\tanh(\hbar\omega_s/2k_BT_s), \qquad (8)$$

where n is the number of nuclei per unit volume. Assuming a Lorentzian lineshape for the nuclear resonance, we can write[14]

$$\chi''(\omega) = \gamma T_2 M_o/2[1 + (\omega - \omega_s)^2T_2^2], \qquad (9)$$

where T_2 is the spin-spin relaxation time.

The general expression for the spectral density of Nyquist voltage noise produced by the spin resistance R_s is given by:

$$S_V^s(\omega) = (\hbar\omega/\pi)R_s\coth(\hbar\omega/2k_BT_s). \qquad (10)$$

Combining Eqs. (8)-(10) with $R_s = 4\pi\chi''\omega L_p\xi$ and neglecting terms of order $(\omega - \omega_s)/\omega_s << 1$, we obtain

$$S_V^s(\omega) = \xi L_p n\hbar^2\gamma^2\omega_s^2T_2/[1 + (\omega - \omega_s)^2T_2^2]. \qquad (11)$$

Hence, the spectral density of the spin fluctuations is centered at the resonance frequency, with an amplitude that is, remarkably, independent of temperature.

Our experiments were performed on 0.63 cm^3 of powdered $NaClO_3$, with a filling factor of about 35%. The ^{35}Cl nucleus has a NQR transition frequency of 30.6856 MHz, while $T_2 = 240$ μs. We performed two separate experiments. In the first, the spins were allowed to reach thermal equilibrium with the helium bath ($T = T_s$), which was at 1.5K. The spin-lattice relaxation time T_1 had been reduced to 20 min by γ-ray irradiation. In the thermal limit $\hbar\omega << k_BT$, the spectral density of the current noise in the input circuit is

$$S_I(\omega) = \frac{(2/\pi)k_BT[R_i + R_s(\omega)]}{[R_i + R_s(\omega)]^2 + [\omega[L_i + L_s(\omega) + L_p] - 1/\omega C_i]^2}. \qquad (12)$$

When the input circuit is tuned to the spin frequency ($f_o = f_s$), Eq. (12) reduces approximately to $2k_BT/\pi[R_i + R_s(\omega)]$ on resonance, so that the effect of the spins is to produce a "dip" in the spectral density. A representative example of our experimental data, averaged over 3 hours, is shown in Fig. 5. The ^{35}Cl resonant fre-

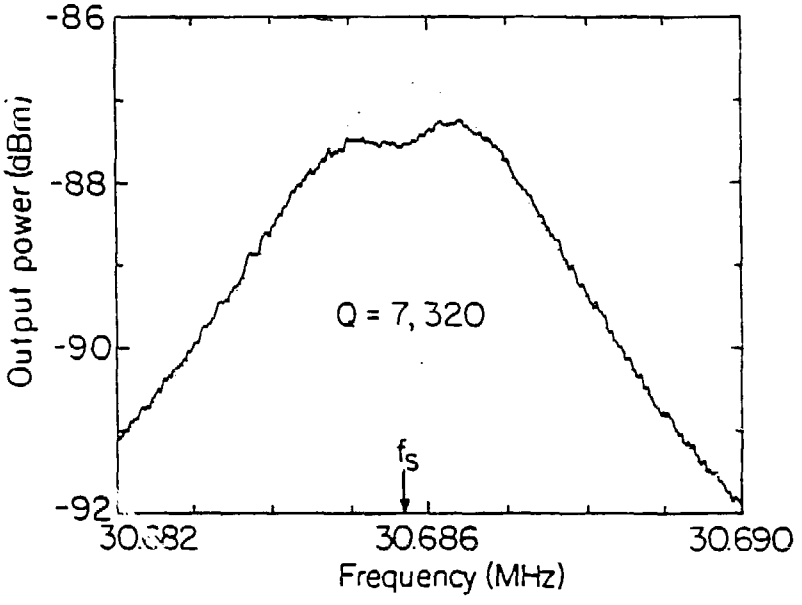

Fig. 5: Spectral density of noise current in the presence of a $NaClO_3$ sample in thermal equilibrium at 1.5K.

quency f_s measured in a separate, pulsed NQR experiment at the same temperature is indicated by an arrow. We observe a dip in the spectral density centered at f_s, which arises from the peak in $R_s(\omega)$ at f_s. We have fitted the data to Eq. (12), allowing Q, R_s, f_s, and T_2 to vary. We find f_s = 30.68565 MHz and $\Delta f_s = 1/\pi T_2$ = 1.3 kHz, in excellent agreement with the values measured separately, while Q = 7,320 and R_s/R_i = 0.14. The dotted line in Fig. 5 indicates the response we would expect from this fit in the absence of the sample.

In the second experiment we use a non-irradiated sample with a T_1 of about 1 week. We equalize the spin populations of the ground and excited states by applying a continuous rf signal at frequency f_s for a few minutes. For zero population difference, the net magnetization, susceptibility and spin resistance R_s are zero, while the spin temperature T_s is infinite. However, because of the temperature independence of Eq. (11), R_sT_s remains constant, equal to the value in the equilibrium state. After the rf signal is removed, the population difference remains zero for a time short compared with T_1. Thus, the spectral density of the current becomes

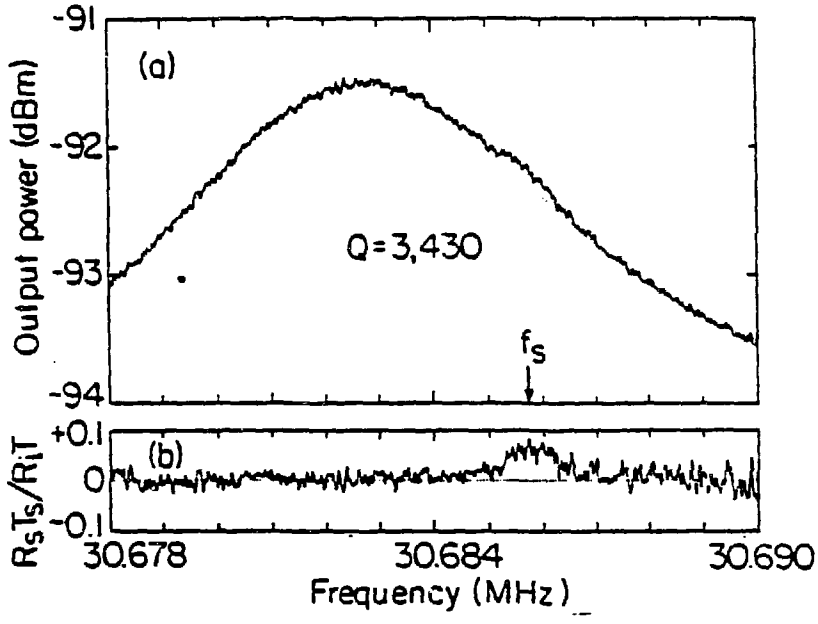

Fig. 6: Spectral density of (a) noise current in the presence of a saturated $NaClO_3$ sample ($T_s \to \infty$), and (b) nuclear spin noise of $NaClO_3$ sample obtained from (a).

$$S_I(\omega) = \frac{(2/\pi)k_B[TR_i + T_sR_s(\omega)]}{R_i^2 + [\omega(L_i + L_p) - 1/\omega C_i]^2} \quad . \tag{13}$$

Thus, we expect to observe a "bump" in the spectral response due to the nonequilibrium contribution T_sR_s to the noise.

An example of our data, averaged over 7 hours, is shown in Fig. 6(a), with the spin resonant frequency indicated with an arrow. Fitting the data with the values of f_s and Δf_s obtained in the first experiment, we find $Q = 3,430$ and $R_sT_s/R_iT = 0.06$. The dotted line indicates the expected spectral density in the absence of a sample. Figure 6(b) shows the excess noise observed in Fig. 6(a) due to the spins. The bump at f_s represents the first observation of nuclear spin noise, and arises from the decay of the nonequilibrium state via spontaneous emission into the circuit.

Acknowledgement

This work is supported partially by the Director, Office of Energy Research, Office of Basic Energy Sciences, Materials Sciences Division of the U.S. Department of Energy under contract No. DE-AC03-76SF00098 and partially by the National Science Foundation under contract DMR83-08082.

References

1. Hirschkoff, E.C., O.G. Symko, L.L. Vant-Hull, J.C. Wheatley. 1970. J. Temp. Phys. 2, 653.

2. Bishop, J.H., E.C. Hirschkoff, J.C. Wheatley. 1971. J. Low Temp. Phys. 5, 607.

3. Day, E.P. 1972. Phys. Rev. Lett. 29, 540.

4. Meredith, D.J., G.R. Pickett, O.G. Symko. 1973. J. Low Temp. Phys. 13, 607.

5. Webb, R.A. 1977. Rev. Sci. Instrum. 48, 1585.

6. Chamberlin, R.V., L.A. Moberly, O.G.Symko. 1979. J. Low Temp. Phys. 35, 337.

7. Suzuki, H., Y. Higashino, T. Ohtsuka. 1980. J. Low Temp. Phys. 41, 449.

8. Pickens, K.S., D.I. Bolef, M.R. Holland, R.K. Sundfors. 1984. Phys. Rev. B 30, 3644.

9. Ehnholm, G.J., J.P. Ekstrom, M.T. Loponen, J.K. Soini. 1979. Cryogenics 19, 673.

10. Wennberg, A.K.M., L.J. Friedman, H.M. Bozler. 1984. Physics 126 B+C, 265.

11. Hilbert, C., J. Clarke. 1983. Appl. Phys. Lett. 43, 694; 1985. IEEE Trans. Magn. 21, 1029; 1985. J. Low Temp. Phys. 61, 3/4.

12. Bloom, M., E.L. Hahn, B. Herzog. 1965. Phys. Rev. 97, 1699.

13. Hilbert, C., J. Clarke. 1984. Appl. Phys. Lett. 45, 799.

14. See for instance, Slichter, C.P. 1984. Principles of Magnetic Resonance. Springer, New York.

DISCLAIMER